UNIVERSITEIT VAN AMSTERDAM

VU VRIJE UNIVERSITEIT AMSTERDAM

Bachelor Thesis Physics and Astronomy

Properties of 2D TiB_2 as candidate for friction and wear resistant coating material

A DFT study

By:

Christian Mirone

Conducted between April 2, 2024, and July 1, 2024

Abstract

Density functional theory (DFT) was employed to examine whether 2D TiB_2 would make for a good candidate for hard coatings in order to reduce energy consumption. Around 20% of the worlds energy consumption every year is caused by friction related processes. To do this we calculated the formation energies of the material, B and Ti vacancies, B_{Ti} and Ti_B antisites, the adsorption energies of H_2, O_2 and H_2O and the binding energies of multiple stacked TiB_2 layers. The used functionals were PBE (bulk) and optPBE-vdW (2D systems). The calculated formation energy for 2D TiB_2 was E_{form}= 0.26 eV/atom, which means that 2D TiB_2 will not form by itself and has to be made under certain conditions. The mechanical properties showed an increase in strength when adding layers on top of the monolayer. From G= 104.47 Nm^{-1} and E= 223.60 Nm^{-1} to G= 161.59 Nm^{-1} and E= 355.46 Nm^{-1} when adding 4 additional layers for the shear and Young's modulus respectively . The density of states (DOS) slightly changes when going from bulk to 2D. The formation energies of B and Ti vacancies for a 2D structure consisting of 108 atoms (6x6x1 cell) were 0.99 eV and 1.23 eV respectively. The energy needed to form B_{Ti} and Ti_B antisites were 1.34 eV and -0.19 eV respectively. This negative value is probably caused by how the chemical potentials were calculated. O_2 has a strong adsorption on the Ti side of -11.24 eV. The adsorption of O_2 could be reduced by letting the B side face the air in a structure since it has a lower adsorption energy, or by adding an hexagonal boron nitride layer on top of the structure. The binding energies showed that at around 29 layers the 2D structure would start to resemble the bulk one. Our findings indicate that TiB_2 could be a candidate for 2D hard coatings if the adsorption of O_2 is reduced and if the structure consists of less than 29 layers.

Student number: 13926071
Research institute: Advanced Research Center for Nanolithography (ARCNL) and Institute of Theoretical Physics (ITFA)
Research group: Materials
Supervisor: Emilia Olsson
Examiner: John Sheil

1 Nederlandse samenvatting

In dit onderzoek hebben we gekeken naar 2D Titanium Diboride (TiB_2) voor mogelijke applicaties als slijtage- en wrijvingsbestendige coating. Dit is gedaan met het idee om de energie consumptie van bepaalde mechanische processen te verminderen.

Iedere jaar wordt gemiddeld 20% van de wereld energie consumptie verspilt door wrijving en wrijving gerelateerde processen. Dit zou verminderd kunnen worden door gebruik te maken van een frictie reducerend coating. Dit onderzoek is gedaan met behulp van Density Functional Theory (DFT) wat voornamelijk gebruikt wordt om de elektronische structuren van materialen te berekenen. Met deze informatie kunnen we veel meer eigenschappen van een materiaal bepalen.

TiB_2 is gekozen als kandidaat doordat het als bulk materiaal (veel 2D lagen op elkaar) een hoge slijtage resistentie, smelt punt, hardheid en een goede geleider is. 2D materialen zijn opgebouwd uit enkele atomaire lagen en tonen verschillende eigenschappen dan bulk materialen omdat ze voornamelijk uit oppervlakte bestaan. Door meerdere lagen TiB_2 op elkaar te plaatsen kunnen we een structuur maken die sterke bindingen heeft in de x en y richting maar zwakke bindingen heeft tussen de lagen (z richting), dit zou het mogelijk moeten maken om de lagen over elkaar heen te laten glijden waardoor de frictie gereduceerd kan worden.

Om te bepalen of 2D TiB_2 gebruikt zou kunnen worden hebben we naar verschillende eigenschappen gekeken voornamelijk, de energie die het kost om een 2D laag te maken, de energie nodig om defecten te introduceren, hoe graag een laag verschillende moleculen zoals H_2, O_2 en H_2O adsorbeert, hoe sterk 2D TiB_2 is en bij welke hoeveelheid lagen we van een 2D materiaal naar een bulk materiaal gaan. De verschillende formatie energieën geven aan of het materiaal stabiel is terwijl de adsorptie energieën zijn nodig doordat geabsorbeerde atomen op een 2D laag de frictie en slijting kunnen laten toenemen en dus is het belangrijk om te weten hoe vaak/makkelijk dit gebeurd.

De resultaten van de formatie energieën tonen ons dat 2D TiB_2 niet uit zichzelf zal vormen doordat het een positieve waarde heeft (0.26 eV/atom). Dit betekend dat we 0.26 eV aan energie per atoom in een systeem zouden moeten stoppen voordat het zal vormen. Voor de defecten in een 2D structuur kost het 1.23 eV om een Ti atoom te verwijderen, 0.99 eV om een B atoom te verwijderen, 1.34 eV om een Ti atom te vervangen met een B atoom en -0.19 eV om een B atoom te vervangen met een Ti atoom. Al deze positieve waardes laten zien dat het energie kost om deze defecten te maken en dus niet uit zichzelf zullen ontstaan, behalve om een B atoom vervangen met een Ti atoom. De reden waarom dit waarde negatief is komt waarschijnlijk door de manier waarop sommige begin waardes voor de berekeningen gekozen zijn.

De mechanische eigenschappen tonen ons dat 2D TiB_2 snel in kracht toeneemt wanneer lagen op elkaar in de AA configuratie (oftewel Ti atomen op Ti atomen en B atomen op B atomen). Bij 29 lagen zal een structuur van TiB_2 van 2D naar bulk (3D) gaan waardoor we de schuif mechanisme tussen de lagen verliezen en dus frictie toe zal nemen.

De adsorptie energieën laten ons zien dat O het makkelijkste atoom is om te adsorberen voor TiB_2, beide aan de B kant (-3.02 eV) en de Ti kant (-5.64 eV). Dit betekend dat zuurstof vrijwel altijd geadsorbeerd zal worden als het zich in een omgeving bevindt met TiB_2. Om dit tegen te gaan kan er een laag hexagonale boron nitride aan het 2D structuur toegevoegd worden doordat deze weinig interacties aangaat met andere moleculen en atomen.

In conclusie, de resultaten tonen ons dat een 2D TiB_2 coating wel theoretisch gezien mogelijk is om te maken. Het is stabiel genoeg dat het niet vanuit zichzelf uit elkaar valt, het is redelijk sterk en het kan sterker gemaakt worden bij gebruik van meerdere lagen. Er zijn echter een paar eisen waar het materiaal aan moet voldoen. Er moet een beschermend laag zijn die de adsorptie van atomen tegenhoudt en het moet uit minder dan 29 lagen 2D TiB_2 bestaan.

Contents

2 Introduction

The discovery of graphene (2D carbon monolayer) has sparked entire new research fields and revolutionized others [1]. Because of them mostly being surface, two-dimensional (2D) materials show novel and unusual physics [2]. 2D materials provide great versatility in tuning their properties. In addition, different 2D materials can be stacked to form heterostructures (fig: 1), where not only their original characteristics are retained but they can also outperform them [3] [4]. For example, 2D semiconductors are often used for water splitting. Problems arise however when a single 2D semiconductor is used. Because of it consisting of only surface, oxidation and reduction reactions restrict each other since they occur on the same surface. This problem can be improved by separating the reactions at different layers with the use of heterostructures [4]. Field-effect transistors (FET) are another example where heterostructures could outperform current technologies due to their good electrostatics [5].

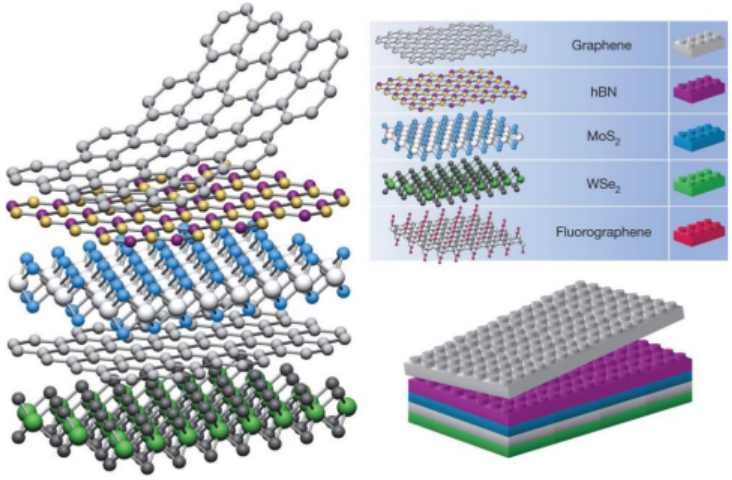

Figure 1: Different 2D materials stacked to form an hetrostructure. 2D materials can be seen as atomic scale building blocks, where different combinations of them result in different properties. Picture adapted from [6].

2D monolayers can be used to make also different structures like MXenes, TMDs and MBenes. MXenes are one of the most recently synthesized 2D materials [7]. They are produced by selectively etching out layers from a precursor material called MAX phase with a general formula of $M_{n+1}AX_n$ which consist of a transition metal (M), an A-group element (A), and carbon or nitrogen (X)[7]. Due to their specific 2D structure and metal sites MXenes perform great in energy storage and catalytic applications. Transition metal dichalcogenides (TMDs) exhibit unique electronic, optical, and mechanical properties, making them useful in various applications such as electronics, photonics, catalysis, and energy storage. Their formula is MX_2 where M is a transition metal and X is a chalcogen, and consist of three stacked layers X-M-X. And lastly the MBenes. Transition metal borides (MBenes) have been predicted by theoretical calculations, recently, as optimal alternatives for different applications, such as metal-ion batteries, catalysts and coatings for surfaces. While MBenes have been extensively researched in their bulk form, investigations into their low-dimensional counterparts, such as nanoflakes, nanosheets, and nanotubes, are still in their early stages of development [8]. Titanium di-boride (TiB_2) is one such MBene.

TiB_2 is a well known ceramic material with high strength to density ratio, wear resistance, melting point, hardness and electrical conductivity [9]. It crystallises in the $P6/mmm$ space group and has the structure of a AlB_2-type metal boride, meaning it consists of an hexagonal B sheet with Ti atoms placed at the center of the hexagons (see fig. 5 section 3.3). A unit cell consists of one Ti atom and two B atoms. TiB_2 is commonly used as armor material for military application, coating to reduce friction between two surfaces and aerospace material due to its high thermal stability. However, little research has been conducted on how the material properties of bulk TiB_2 (b-TiB_2) translate to a single monolayer (m-TiB_2). Zhang *et al* [10] demonstrated that m-TiB_2 is an energetically and dynamically stable Dirac material. Sharma *et al* [8] recently have shown that m-TiB_2 has high transition probabilities at the Dirac point which are tunable by spintronic effects. Thus, suggesting that m-TiB_2 has a great potential for spintronic and optoelectronic applications. Sevik *et al* [11] showed that high temperature superconductivity can be achieved by means of doping in the boron honeycombed layer in similar materials (V, Ta, Sc, Ca, Nb) B_2. Other works reveal the nitrogen adsorption capabilities of vacant sites in delaminated TiB_2 nanosheets possibly leading to the use of TiB_2

nanosheets for nitrogen fixation [8].

There exist various techniques to synthesize 2D metal borides. Chemical and mechanical exfoliation are two of these were the synthesis of $m\text{-}TiB_2$ has been proven possible. Chemical/liquid-phase exfoliation works by weakening the bonds that hold the stacked metal borides together with a solvant, this delaminates the stacked metal into multiple 2D structures. This is usually done with metal borides with the AlB_2 structure. To achieve high quality and yield, the right solvant medium has to be used [12]. Mechanical exfoliation is a technique used to isolate thin layers or flakes from a bulk material through mechanical means. Current research findings suggest that ball milling and mechanical grinding can be used as mechanical methods to exfoliate metal borides such as TiB_2, NbB_2, MgB_2 and VB_2 [12].

This research aims to shine new light on 2D MBenes, in particular $m\text{-}TiB_2$, for tribological applications as wear and friction reducing coatings to reduce the energy usage of certain mechanical processes. While MXenes and TMDs could have also been chosen for this research MBenes may have stronger in plane bonds due to the hexagonal B-layer and are still quite new meaning not a lot is known about them [13].

Friction is present in nearly all mechanical systems and is a major cause of mechanical failures, inefficiencies and energy loss. Studies have shown that an estimated 20% of the worlds energy consumption every year is caused by friction and friction related phenomena [14]. To reduce friction is to reduce the energy consumption of a process. Liquid lubricants have been the main way of reducing friction for a long time. They however, can have an undesirable impact on the environment and multiple efforts have been implemented to reduce their usage [14]. Tribology (the study of friction), is one of the scientific fields that have been revolutionized since the discovery of graphene. Studies have shown that 2D materials with one or a few atomic layers can reduce the coefficient of friction below 0.01, which is in the regime of superlubricity. Because of the weak interlayer forces and strong covalent in-plane forces the layers are allowed to slide over each other with relatively low friction (see fig.2) [14] .

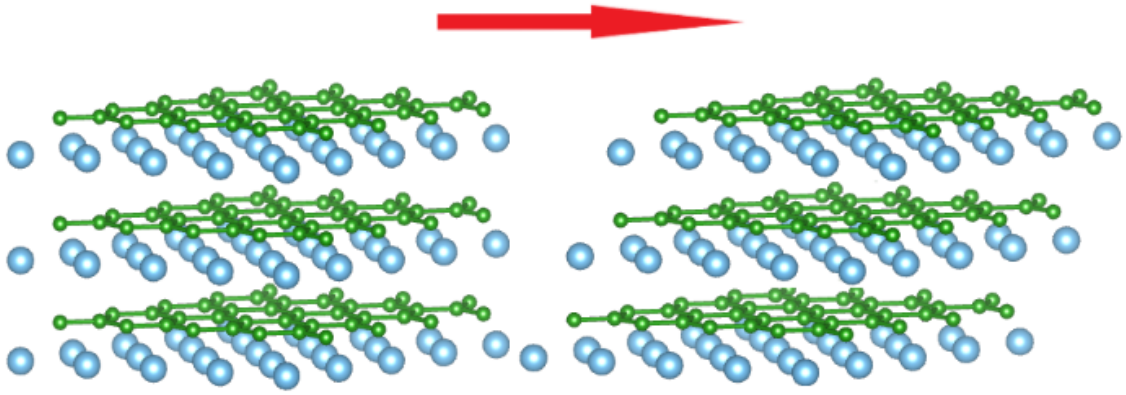

Figure 2: Shifting structure. Because of the weak interlayer binding energies the layers and strong in plane bonds the structures can shift around. When used as a coating this process can reduce friction between two sliding surfaces.

Density functional theory (DFT) was used to conduct this research. DFT has been the mainstay way of calculating electronic structures in solid-state physics for a long time. DFT has drastically reduced computational costs by having the electron density as its fundamental variable instead of a many body wave function. This made it possible to approach larger systems without losing much accuracy compared to previous methods [15]. The foundation of DFT is based on the Honenberg-Kohn theorem, the Kohn-Sham equation and the exchange correlation functionals [16]. The exchange correlation functionals are a fundamental quantity for DFT calculations. Changing the functional means changing the assumptions made on the system, which can lead to different quantities when applying for example two different functionals on the same system. While it being very effective for calculating electronic structures, it is not directly possible to conduct tribological studies with DFT, and even if there was it would have been too advanced for a bachelor thesis. To see whether $m\text{-}TiB_2$ makes for a good candidate as friction reducing coating we firstly investigated the stability of it by looking at formation energies, defects and adsorptions. Secondly, the assumption was made

that if the properties of a structure converged quickly to the $b\text{-}TiB_2$ ones, the material would not make for a good lubricant coating since it would indicate to strong binding energies between monolayers which would make it difficult for them to slide over each other and thus reduce friction.

In this research, we investigated how the properties of $b\text{-}TiB_2$ translate to $m\text{-}TiB_2$ by comparing formation energies, mechanical properties, electronic structures and defects in order to use it as a coating to reduce the energy consumption caused by friction in certain mechanical processes.

3 Method and Theoretical background

3.1 DFT

DFT, as mentioned in the introduction, is commonly used to calculate the electronic structures of systems and properties of materials. Its basics consist of the Boron-Oppenheimer approximation, the Hohenberg-Kohn theorem and the Kohn-Sham equation. The electron density $\rho(\mathbf{r})$ (depends on three coordinate variables) is used as the fundamental variable in DFT calculations [16].

The Born-Oppenheimer approximation states that because of the large difference in mass between nuclei and electrons the electron and nuclear motions can be treated separately, thus splitting the Schrödinger equation into the electron and the nuclear part (see [16] for equations).

The first part of the Hohenberg-Kohn theorem states that the external potential of the system corresponds one-to-one with the ground-state electron density. Meaning that once the ground-state electron density has been determined, the external potential and the physical properties associated with the ground state can be calculated as well [16]. The second part of the theorem states that the ground-state electron density can be obtained by searching for the electron density which minimizes the energy functional:

$$E_v[\rho] = E_{kin}[\rho] + \int \rho(\mathbf{r})v(\mathbf{r})d\mathbf{r} + E_{ee}[\rho] \tag{1}$$

which satisfies:

$$E_v[\rho] \geq E_v[\rho_0] = E_0 \tag{2}$$

where ρ_0 is the ground-state electron density under some external potential $v(\mathbf{r})$. The problem with this function is that $E_{kin}[\rho]$ and $E_{ee}[\rho]$ are unknown [16].

Kohn and Sham proposed a solution to this problem which could give results with sufficient accuracy for practical use. The Kohn-Sham equation is characterized by a local effective external potential (Kohn-Shan potential $v_{eff}(\mathbf{r})$), which can be calculated with eq.4, within which the non-interacting particles are situated. This non-interacting system is described by single particle Schrödinger equation (Kohn-Sham eq. 3) which is the equation for a Kohn-Sham orbital (ϕ_i) in the lattice potential ($v_{eff}(\mathbf{r})$).

$$[-\frac{\hbar^2}{2m}\frac{\partial^2}{\partial\mathbf{r}^2} + v_{eff}(\mathbf{r})]\phi_i(\mathbf{r}) = \varepsilon_i\phi_i(\mathbf{r}), \tag{3}$$

$$v_{eff}(\mathbf{r}) = v(\mathbf{r}) + v_H(\mathbf{r}) + v_{xc}(\mathbf{r}), \tag{4}$$

where ε_i is the Kohn-Sham energy eigenvalue associated with the i-th Kohn-Sham orbital, $v_H(\mathbf{r})$ is the Hartree energy of the electron-electron repulsion and v_{xc} which is the exchange correlation potential. Exchange correlation functionals are an approximation to an unknown function that would give exact results to the DFT calculations if found. The exchange correlation potential can be calculated with:

$$v_{xc} = \frac{\delta E_{xc}}{\delta\rho(\mathbf{r})}, \tag{5}$$

where E_{xc} is the exchange correlation energy.

The DFT calculations start with an approximation of the effective potential (v_{eff}). Plugging this value into the Kohn-Sham eq. (see eq. 3) returns the wavefunction of the orbitals. The electron density is calculated by summing over these orbitals,

$$\rho(\mathbf{r}) = \sum_{i=1}^{N} |\phi_i(\mathbf{r})|^2, \tag{6}$$

where N is the number of electrons and i indicates the occupied Kohn-Sham orbital. Being dependant on the electron density v_{eff} can be calculated again and the whole process is repeated until the change in output between the cycles stops [16][17][15].

3.2 Formation energies

To determine whether the material would be able to form, remain stable after formation and to elucidate defect concentration and type, the formation energies of b-TiB_2, m-TiB_2 and defects on them had to be calculated. Three different formation energies were calculated, the material formation energy (E_{form}), the vacancy formation energy (E_v) and the antisite formation energy (E_{A_b}).

A positive material formation energy indicates that it would be unlikely for the material to form by itself and would need an external energy source to form, while a negative formation energy means that the material would probably form by itself if the right atoms are present inside an environment. After formation, the total energy of a system can be calculated, if positive the system would be unstable and fall apart over time. However, if negative the system would remain stable even if the formation energy is positive.

The formation energies of pristine and bulk TiB_2 were calculated with the following equation:

$$E_{form} = E_{TiB_2} - (\mu_B \times N_B) - (\mu_{Ti} \times N_{Ti}), \tag{7}$$

where E_{TiB_2} is the total energy of pristine b-TiB_2 or m-TiB_2, μ_B and μ_{Ti} are the chemical potentials of B and Ti and N_B/N_{Ti} are the total number of B atoms and Ti atoms present in the structure.

Both vacancies and antisites defects had to be tested on m-$TiB2$ to assess how often they would form and determine what kind of effects they would have on the system. For vacancies and antisites, a positive defect formation energy indicates the amount of energy that would have to be put in the system for such defects to form. The vacancy formation energy was calculated with the following equation:

$$E_v = E_{defect} - E_{TiB_2} + (N_i \times \mu_i), \tag{8}$$

where E_{defect} is the total energy of the relaxed defect structure, E_{TiB_2} is the total energy of the relaxed pristine structure, N_i is the total number of atom vacancies present in the structure and μ_i is the chemical potential of the vacancy atom.

The antisite formation energies were calculated with the following equation:

$$E_{A_b} = E_{antisite} - E_{TiB_2} + (N \times \mu_A) - (N \times \mu_B), \tag{9}$$

where $E_{antisite}$ is the total energy of the antisite structure, E_{TiB_2} is the total energy of the pristine structure, $N \times \mu_A$ is the total energy needed to remove N number of A atoms with chemical potential μ_A from the system and $N \times \mu_B$ is the total energy of N B atoms with chemical potential μ_B which replace the A atoms.

3.3 Chemical Potentials

The chemical potentials were used to calculate the different formation energies and adsorptions. For Titanium and Boron the chemical potentials were obtained by calculating the energy per atom of Ti and B in bulk form. This was done by letting the bulk relax and then dividing the total energy of the system by the total number of atoms. Both the cell sizes of the bulks were set to 1x1x1 with cut-off energies of 500eV and 550eV and k-points of 4x4x4 and 3x3x3 for Ti and B respectively. A similar method was used to calculate the chemical potentials of O_2, H_2 and H_2O. Each molecule was placed inside a vacuum of 15x15x15Å and were let to relax. The total energy of each system was then used as its corresponding chemical potential. The cut-off energy for all the systems was set to 500eV and the k-points to 1x1x1. A bulk material was chosen for Ti and B to calculate the chemical potential since TiB_2 is a solid while O_2, H_2 or H_2O were placed inside a vacuum since they are present in gas form in the air.

3.4 Adsorption energy

The adsorption of atoms on the surface of a material can affect its performance as a wear resistant and friction reducing coating. For example, while for graphite the adsorption of O_2 or H_2O in vacuum reduces the friction between surfaces, the adsorption of these gasses in diamond-like carbon (DLC) increases friction [18]. For this reason it is important to know how a material adsorbs certain molecules/atoms on its surface. Here we chose to look at H_2, O_2 and H_2O since they are common molecules present in air. The stronger (more negative) the adsorption energy (E_{ads}) is the easier and faster the atoms get adsorbed. Each material has its different adsorption sites, these had to be selected before calculating the energies. The selected adsorption sites are shown in fig.11.

The following equation was used to calculate the adsorption energies E_{ads}:

$$E_{ads} = E_{TiB_2+i} - E_{TiB_2} - \mu_i, \tag{10}$$

where E_{TiB_2+i} stands for the total energy of the m-TiB_2 with the adsorbed molecule, E_{TiB_2} stands for the total energy of the pristine system and μ_i is the chemical potential of the adsorbed molecule.

3.5 Binding energy

As mentioned in the introduction, the goal of this research is to determine whether structures consisting of m-TiB_2 are a suitable coating to reduce friction between surfaces. One way to see whether TiB_2 could act as a lubricant is to look at its properties as a structure. Since the bonds between the layers are weak, the layers can shift around which could reduce friction between surfaces, thus acting as a lubricant (see fig 2).

The binding energy between layers was calculated with the following equation:

$$E_{bind} = E_{struc} - N \times E_{monolayer}, \tag{11}$$

where E_{struc} is the total energy of the structure, N is the total number of monolayers and $E_{monolayer}$ is the total energy of a monolayer. The weaker (less negative) the binding energy, the easier it is for the layers to shift around while a stronger one (more negative) would make it harder for the monolayers to slide and at a certain point the structure would start to resemble a bulk material.

3.5.1 Different stacking

Different ways of stacking the monolayers can effect the properties of the structure [8]. The m-TiB_2 can be stacked in three different ways, two layers on top of each other without any shift (AA stacking), two layers where Ti atoms are placed on top of B ones (AB stacking) and two layers where the Ti atoms are placed on top of B bridges (bridge stacked) (see figure 3).

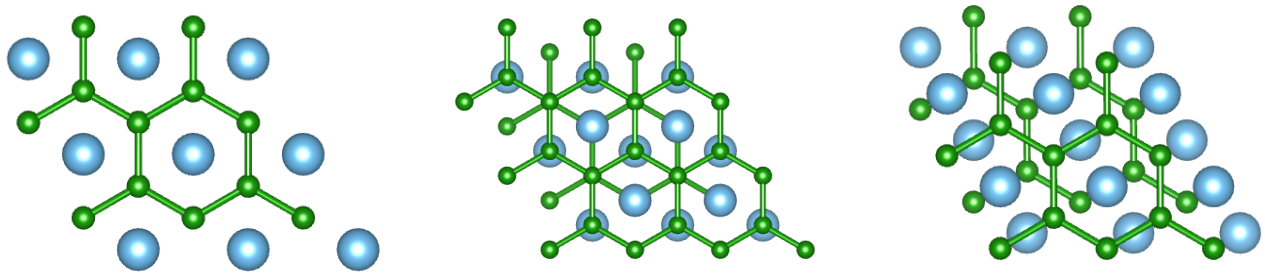

a) b) c)

Figure 3: Different stacking of types of m-TiB_2: a) AA stacked, b) AB stacked, c) bridge stacked. Blue dots are Ti and green dots are B atoms.

The binding energies and intelayer distances were calculated for these stacking types to determine the most stable configuration and to be used as a prediction of how stacked TiB_2 would behave if shifted around. The mechanical properties of the 2 AB stacked and 5 AA stacked layers were also calculated to be compared with m-TiB_2 and b-TiB_2.

Due to time restrictions, it was not possible to calculate the mechanical properties of the other stacking types since the calculations are computationally expensive and thus take a long time to solve.

3.6 Elastic constants

Elasticity describes how a crystal responds to external strain, offering crucial insights into the material's strength as defined by its elastic constants. Young's modulus (E) indicates the material's stiffness in a certain direction, the Shear modulus (G) quantifies the material's response to shear stress, and the bulk modulus (B) describes the materials resistance to uniform compression. The calculation of the elastic constants of a material is essential for understanding its macroscopic mechanical properties. All these properties can be calculated from the elastic constants of the material which define the material's response to different types of deformation. The elastic constants of a material can be calculated with DFT simulations. In this research an elastic package for ASE was used to calculate the elastic constants [19]. The elastic constants of a system can be calculated via Hooke's law:

$$\sigma_i = \sum_{j=1}^{6} C_{ij}\varepsilon_j, \tag{12}$$

Where C_{ij} stands for the elastic constants of the specific components of stress (σ) and strain (ε) in the material [20]. The maximal uniaxial strain was set from -2% to +2% in x and y direction. The lattice constants are fixed and are not allowed to relax while strain is being applied, this assumes that the lattice constant normal to the direction of the strain does not change since the applied strain is small. Small deformations (strains) are applied to a material's cell, next the change in energy for each deformation is calculated which in return gives the force applied. The stress on the system can be calculated by dividing the applied force over the area. Substituting the stress and strain back in Eq.12 gives in return the elastic constants (C_{ij}) of the system.

As previously mentioned, the macroscopic mechanical properties of materials can be calculated using these elastic constants. Only the elastic constants in the x and y directions (i,j= 1 or 2) for 2D structures are taken as physical values while the z direction (i,j= 3) is neglected since the material is 2D. Meaning that while GPa for 3D structures is in terms of Nm^{-2} it is in terms of Nm^{-1} for 2D ones.

The Bulk modulus is calculated during the Equation-Of-States (EOS) calculations. These give the optimal lattice parameters for given systems by changing the lattice parameters and calculating the total potential energy of the system. At the end of the EOS, a Birch-Murnaghan fit [21] returns the lattice parameters of the system with the lowest total potential energy and calculates the bulk modulus of the system. The shear modulus G can be directly derived from the elastic constant C_{66} for both Bulk and 2D TiB_2. Young's modulus (E) for bulk TiB_2 can be derived from the bulk modulus (B) and shear (G) [22]:

$$E = \frac{9BG}{G+3B}, \tag{13}$$

while for 2D TiB_2 it is calculated by using elastic constants:

$$E = \frac{\sigma_{xx}}{\varepsilon_{xx}} = \frac{C_{11}^2 - C_{12}^2}{C_{11}}. \tag{14}$$

Young's modulus, eq. 14, can be derived from Hooks law (eq.12) for plane stress conditions.

The elastic constants can also be used to determine whether the system is stable or not. For a stable hexagonal crystal (bulk) system the stability criteria are: Criteria I: $C_{11} > |C_{12}|$, criteria II: $2C_{13}^2 < C_{33}(C_{11}+C_{12})$, criteria III: $C_{44} > 0$ and criteria IV: C66 > 0. While for a mechanically stable 2D system the criteria are: I: $C_{11} > 0$ and $C_{11} > |C_{12}|$ [8].

3.7 Computational method

The density functional theory (DFT) code GPAW [23] was used for most of the calculations, except for the elastic constants, those were calculated with the Vienna Ab Initio Simulation Package (VASP)[24]. The Perdewe-Burkee-Ernzerhof (PBE) [25] and optPBE-vdW [26] (a combination of the PBE functional and the non-local van der Waals density functional DFT-D3[27]) functionals were used for the calculations. After multiple convergence tests the cut-off

energy was set to 500 eV with varying k-point grids depending on the cell sizes used (see table 1) and a vacuum thickness of 15Å set to reduce the interactions between the monolayers. The convergence criteria for all the calculations in this research was set to 0.01 eV.

3.7.1 GPAW

GPAW is an Atomic Simulation Enviroment (ASE) package used to run DFT calculations based on the projector-augmented-wave (PAW) method. The PAW method makes use of pseudopotentials which describe the nuclei and core electrons with a smoother potential. The Kohn-Sham equation (eq.3) is then solved only for the valence electrons, thus reducing the number of wavefunctions which have to be calculated. PAW also makes use of the augmented-plane-wave (APW) method which devides space into atom-centered augmentaiton spheres. The GPAW package has however drawbacks. By smoothing out the potential near the core electrons all the information close to the nuclei is lost, which can have an effect on the calculations of certain properties such as hyperfine parameters [28].

3.8 Convergence tests

Before running any calculation the convergence criteria (cut-off energy, k-points and vacuum size) had to be determined. PBE was used to calculate the cut-off energy and k-points since it is fast and gives reasonable results, while for the vacuum convergence of the monolayer optPBE-vdW was chosen since vdW interactions are important and optPBE-vdW is a combination of PBE with van der Waals interactions[26].

The cut-off energy was determined first, this was done by calculating the total potential energy of a system for changing cut-off energies with an arbitrarily chosen k-point for the bulk of 4x4x4 for bulk and for the monolayer 4x4x1 togheter with a vacuum size of 15Å. Once the difference between two cut-off energies was smaller than 0.01eV/atom the cut-off energy was considered to be converged. The number of k-points was calculated with the same principle but now with a varying number of k-points and the cut-off energy set to the previously found value. Lastly, the vacuum convergence test was done to determine at what distance two monolayers would not feel each other. Again, the same method as before was used to calculate the vacuum size where the cut-off energy and k-points were set to the converged values and the vacuum was varied (this was only done for the monolayers). The found convergence criteria are shown in table 1.

4 Results

4.1 Convergence test results

The results from the convergence test are shown in the table below 1. Figure 4 shows the convergence test results for a 2x2x1 monolayer. As the cut-off energy values increase the difference in energies decreases. This is also valid for the k-points and vacuum. The first data point is high for each of the figures due to how the difference in energies was calculated. The last value of the list was taken to calculate the difference with the first value, but because at the start the last value is still empty we get a big difference. Hence the first data points can be neglected. Figure 4c shows the vacuum convergence test results. This graph stops at a vacuum of 13Å while the vacuum chosen for the rest of the research was 15Å. The values at 13Å had already converged below the 0.01 eV but a vacuum of 15Å was chosen so other simulations, like adsorptions, could also run without the molecules feeling the effects of the monolayer above.

Table 1: Convergence test results (functional: PBE)

	cell size	cut-off energy (eV)	k-points
Bulk	1x1x1	550	7x7x7
	2x2x2	500	5x5x5
	4x4x4	500	1x1x1
Monolayer	1x1x1	500	5x5x1
	2x2x1	500	4x4x1
	6x6x1	500	1x1x1

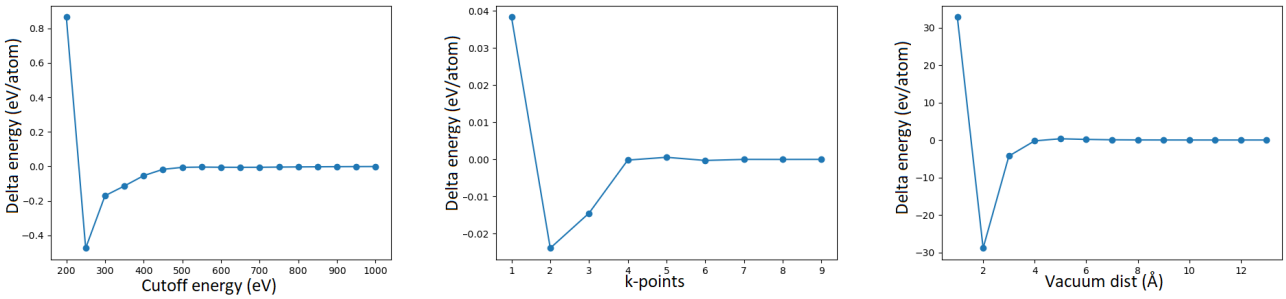

a) b) c)

Figure 4: Convergence results of 2x2x1 monolayer: a) cut-off energy convergence, b) k-points convergence, c) vacuum size convergence.

4.2 Functionals

The right exchange correlation functional had to be chosen before running the calculations. The functional was chosen by comparing the bulk moduli and lattice parameters of different functionals, obtained from the EOS calculations to values found in the literature. The different tested functionals were PBE [25], optB88-vdW [26], BEEF-vdW [29] and optPBE-vdW[26], which were chosen because of them already being implemented in GPAW. Table 2 shows the results of the EOS. Both for the bulk and 2D TiB_2 different functionals give very similar results for the lattice parameters and bulk moduli. Only the ground energy values showed major differences, this because as mentioned in section 2.1 the exchange correlations are approximations of an unknown function that give exact results to DFT calculations. The found lattice parameters a = 3.04Å and c = 3.25Å and bulk moduli for the bulk are in agreement with previously found values (a = 3.029Å, c = 3.229Å, B = 240 GPa)[9]. Also the lattice parameter a=2.98Å and bulk moduli for the monolayer are in agreement with values found in the literature (a = 3.035Å, B = 73.89 GPa)[8]. The bulk modulus is only used as a way to compare the functionals to each other but is further not seen as a physical value for the 2D systems since we ignore the z component.

Since the values gave similar results we were free to choose the functionals. The two chosen functionals were PBE[25] and optPBE-vdW[26]. The PBE functional was used for the bulk systems, since it gives a general good description of bulk materials and is fast. OptPBE-vdW was chosen for the monolayer, this because optPBE-vdW (which is a combination of the PBE functional togheter with the vdW-DF correction method is similar to a functional used in a previous study [30], which looked at the mechanical properties of TiB_2. The study used the DFT-D3 functional which is a combination of the PBE functional together with a vdW-D3 correction[31].

Table 2: Optimized lattice constants a and c, ground energy (E_g) and bulk modulus (B)

	Functional	a (Å)	c (Å)	B (GPa)
1x1x1 Bulk	PBE	3.04	3.25	262.34
	BEEF-vdW	3.04	3.25	262.27
	optB88-vdW	3.04	3.25	258.78
	optPBE-vdW	3.04	3.25	254.17
Previous studies [9]	experimental	3.03	3.23	240.00
1x1x1 Monolayer	PBE	2.98	15	93.36
	BEEF-vdW	2.98	15	93.49
	optB88-vdW	2.98	15	93.35
	optPBE-vdW	2.98	15	92.49
Previous studies [8]	PBE	3.04	15	73.89

4.3 Bulk & Monolayer characteristics

The bond lengths between Ti and B atoms of m-TiB_2 are l_{Ti-B} = 1.74Å and between B atoms l_{B-B} = 2.20Å while the distance between the B and Ti layer is h = 1.34Å. These values come close to previously found ones, l_{Ti-B} = 2.38Å, l_{B-B} = 1.75Å and h = 1.19Å [8]. The small difference between values may be caused by the different functionals used between papers. The bond lengths of b-TiB_2 are l_{Ti-B} = 2.39Å, l_{B-B} = 1.76Å and h = 1.62Å, which also come close to previous found values l_{Ti-B} = 2.35Å, l_{B-B} = 1.75 [32]. The vertical distance between Ti atoms and B layer is significantly smaller for the monolayer, indicating a stronger interaction between the two in respect to the bulk[10].

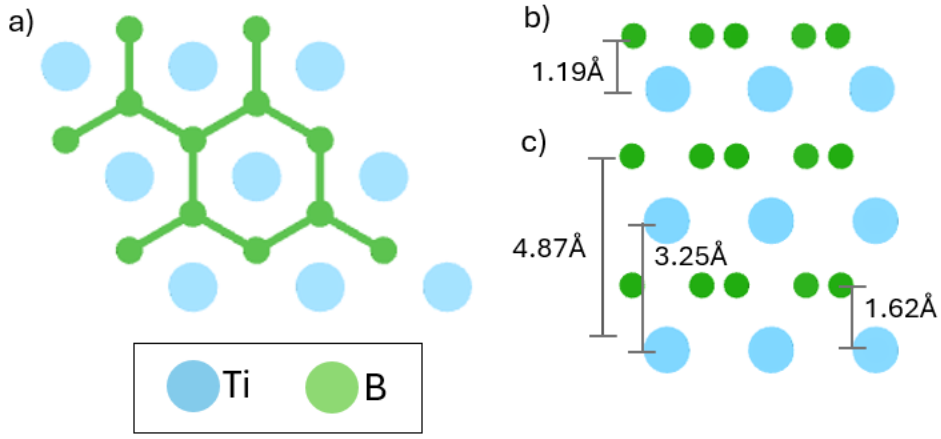

Figure 5: a) Top view of TiB_2 structure, b) side view of m-TiB_2 and c) side view of b-TiB_2.

4.3.1 Formation energies

Like previously mentioned in section 2.3, the formation energies indicate whether a material is able to form in the applied conditions. The formation energies were calculated with Eq.8. Both the functionals PBE and optPBE-vdW were tested for both bulk and monolayer TiB_2. The formation energies are shows in table 3.

Table 3: Table of formation energies (E_{form}) for bulk and monolayer TiB_2

	Functional	E_{form} (eV/atom)
Bulk	PBE	-1.06
	optPBE-vdW	-1.03
Monolayer	PBE	0.23
	optPBE-vdW	0.26

Both functionals return similar formation energies. The bulk formation energies are negative, meaning that the compound is stable and likely to form spontaneously releasing energy in the process. While the formation energies of the monolayer are positive. You would have to provide around 0.26 eV per atom for the material to form. However the total energies of all the systems were negative. Indicating that the material remains stable after formation.

4.3.2 Mechanical properties

As mentioned in section 2.7 another way of telling whether a material is stable is through elastic constants. Table 4 shows the found elastic constants together with the bulk modulus (B), Young's modulus (E) and shear modulus (G). Figure 6 shows the EOS fit of b-TiB_2 together with the calculated B.

The mechanical stability criteria have been fulfilled by all the structures thus indicating their stability. The values found for the elastic constants of b-TiB_2 and m-TiB_2 come close to the values found in other studies [8][33]. Comparing the values of the m-TiB_2 to the bilayer structures shows an increase in strength (AA > AB > m-TiB_2), this increase in stiffness can be mainly attributed to the presence of interlayer interactions in the bilayers [8]. AA stacked TiB_2 seems to be stronger than AB stacked, this aligns with the results shown by Sharma *et al* that AA

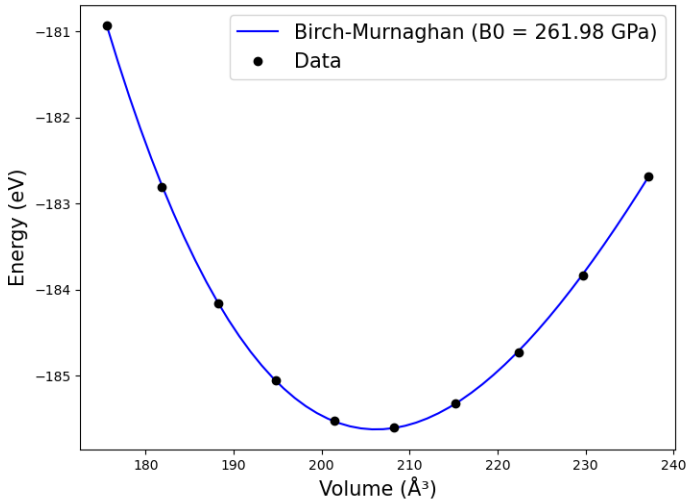

Figure 6: EOS fit of b-TiB_2 with calculated bulk modulus (B) of 261.98 GPa.

Table 4: Table of elastic constants of monolayer (Nm^{-1}), bilayer (Nm^{-1}),5 layers (Nm^{-1}) and bulk (GPa) together with equivalent mechanical properties bulk (B), shear modulus (G) and Young's modulus (E).

	Structure	C_{11}	C_{12}	C_{13}	C_{22}	C_{33}	C_{44}	C_{66}	B	G	E
This study	b-TiB_2	604.19	86.95	108.70	607.19	432.34	236.05	257.01	261.98	257.01	581.03
	m-TiB_2	122.49	5.24	-1.51	153.35	0.86	-1.63	67.15	—	67.15	122.27
	AB bilayer	225.83	22.44	1.19	223.11	2.32	7.56	104.47	—	104.47	223.60
	5 AA layers	359.25	36.89	1.40	360.99	9.32	9.26	161.59	—	161.59	355.46
Other studies	b-TiB_2[33]	656.00	65.00	98.00	—	461.00	262.00	—	250.30	260.70	581.00
	m-TIB_2[8]	170.92	-23.14	—	—	—	—	—	73.89	97.03	167.78
	AA bilayer[8]	327.26	72.62	—	—	—	—	—	199.94	127.32	311.14

stacked bilayers are stronger and more stable than AB ones [8]. When comparing the AA bilayer structure to the 5 AA layers we see a small increase in C_{11}, G and E. This indicates that the rate at which the mechanical strength increases is not linear. Sharma *et al* [8] also reported that m-TiB_2 and AA-stacked m-TiB_2 have a brittle nature which can be drastically reduced by adding additional layers. The values found in our structures seem to be slightly different from the values found in other studies, mainly the value for C_{12}. This is probably caused by the different assumptions made when strain is applied to the system. As mentioned in section 2.7, we fix the lattice parameters when applying strain while they let the lattice parameters change [8]. This results in an auxetic behaviour (negative Poisson's ratio) present in m -TiB_2 which is rare for 2D materials and is not present in our results. This auxetic behaviour is quickly lost when adding additional layers to the monolayer [8]. Free standing m-TiB_2 has a bending instability. A monolayer will slowly turn into a tubular structure if left alone, meaning that free standing m-TiB_2 needs to be stabilized on a substrate such as h-BN for applications as a single monolayer [34].

4.3.3 Electronic properties

The calculated density of states (DOS) and the projected density of states (PDOS) of b-TiB_2, m-TiB_2 and AA stacked m-TiB_2 are shown in figure 7. The PDOS shows the distribution of electrons for each different shell while DOS is the total sum of all the different PDOS. As mentioned in the introduction, multiple articles report m-TiB_2 being a Dirac material [34]. However, figure 7b shows no signs of Dirac states near the Fermi level, this is probably caused by the functional used optPBE-vdW that includes the PBE functional which is well known for underestimating band gaps [35], while in the paper the HSE functional was used which is more accurate for electronic structures. According to Sharma *et al* [8], the Dirac states are lost when an additional layer of m-TiB_2 is added onto the monolayer. The AA stacked system shows a metallic nature and resembles more the bulk structure. Ti(d) and B(p) have the highest

contributions near the Fermi level. This indicates that the system is held together by covalent bonds between the Ti and B atoms.

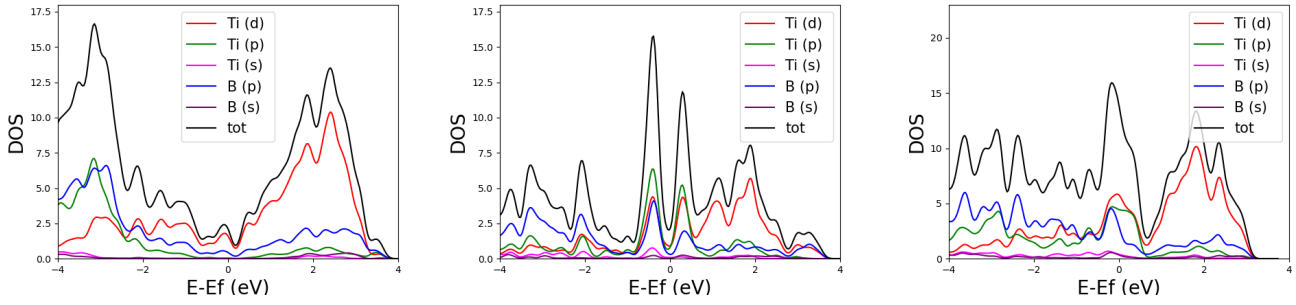

a) b) c)

Figure 7: Total and projected density of states for pristine a) bulk, b) monolayer and c) AA stacked TiB_2. total DOS is the sum of all structures. Black line is the total DOS while colored lines are the PDOS.

4.4 Defects

Defects can impact the mechanical and electrical properties of a material, hence it is important to know their formation energies to estimate how often they form. Knowing what kind of effects defects have on the properties of a material helps to understand the overall material behaviour. Additionally, this knowledge can be used to willingly change or enhance the material's properties.

4.4.1 Vacancies

We tested the effects of vacancy defects on m-TiB_2 and b-TiB_2. Different cell sizes were used to simulate changing defect densities. Each cell had a single vacancy of either B or Ti. The results are shown in table 5.

Table 5: Formation energies (eV) of Ti and B vacancies and B_{Ti} and Ti_B antisites. The monolayer and bulk values were calculated with optPBE-vdW and PBE respectively.

	2x2x1 (12 atoms)	3x3x1 (27 atoms)	4x4x1 (48 atoms)	5x5x1 (75 atoms)	6x6x1 (108 atoms)	bulk
E_{Ti}(eV)	1.59	1.65	1.76	1.34	1.23	4.98
E_B(eV)	0.72	—	1.78	1.38	0.99	3.05
$E_{B_{Ti}}$(eV)	—	—	—	—	1.34	8.88
E_{Ti_B}(eV)	—	—	—	—	-0.19	8.73

Starting from a 2x2x1 cell the formation energies seem to increase up to the 4x4x1 cell and then decrease again (see table 5). A bulge of around 1Å forms when removing a B atom from the 6x6x1 structure (see fig. 8a). This bulge is also present in the 5x5x1 cell but is smaller and is not present in the 4x4x1 cell. The lack of bulge in the 4x4x1 cell is probably caused by the size of the cell during relaxation. Because of the small size of the cell the atoms cannot relax properly thus impeding the bulge to form. Because the cell is small at 4x4x1 the B vacancies will feel each others effects, thus increasing the formation energy of the defects. This makes it harder for B vacancies to form close to each other. This bulging effect is also present in the 5x5x1 cell when removing Ti atoms, but is smaller (around 0.26Å). It however, is not present in the 6x6x1 cell (see fig. 8b). This shows that Ti vacancies have a smaller impact on the structure deformation than B vacancies. Near a vacancy the atoms are pulled in closer together to compensate for the charge difference and to minimize the total energy of the system. This leads to smaller bond lengths between the local atoms thus causing the bulge to form. When looking at the formation energies of B vacancies in the 6x6x1 monolayer, we see that ,like in the bulk, it is easier for them to form than Ti ones.

The electronic structures of the systems slightly change when Ti or B atoms are removed. Compared to the pristine structure (fig. 9a) the peaks of the B vacancy DOS (fig. 9c) become lower and broader. This is probably caused by the redistribution of the charges. The peak present at around 2 eV for the pristine sheet merges with the peak at around 1 eV when B and Ti are removed. The overall changes of the electronic structure are negligible.

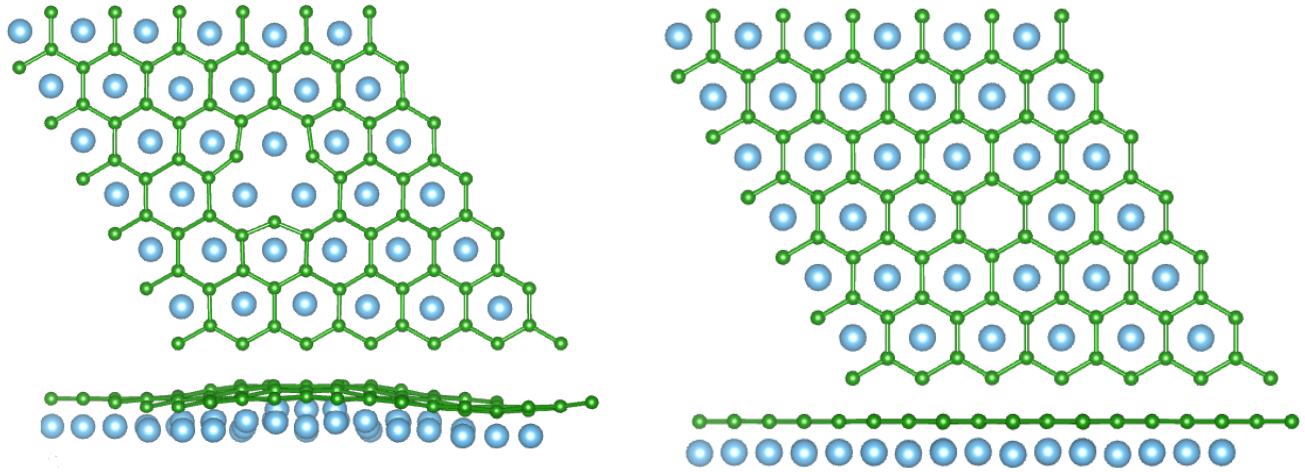

a) b)

Figure 8: Vacancies on a 6x6x1 monolayer of TiB_2. a) B vacancy, b) Ti vacancy. The bulge present in fig.a is caused by the redistribution of the charge around the defect.

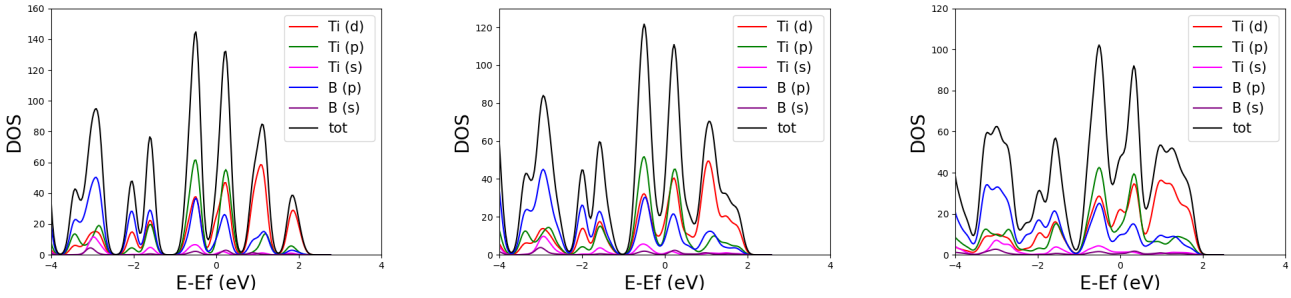

a) b) c)

Figure 9: Effects of B and Ti vacancies on a 6x6x1 pristine monolayer. a) Pristine monolayer, b) Ti vacancy, c) B vacancy. The overall changes on the electronic structures are negligible.

4.4.2 Antisites

The formation energies for B_{Ti} and Ti_B antisites are also shown in table 5. For a 6x6x1 cell an energy of around 1.34 eV is needed for a B atom to replace a Ti atom (B_{Ti}), this means an external energy source is needed for this antisite to form. Unlike for B_{Ti}, the formation energy of a Ti_B antisite is negative (E_{Ti_B} = -0.19 eV). This would mean that this process would happen spontaneously releasing -0.19 eV of energy each time which destroys the TiB_2 monolayer. This negative value is probably a result of the chosen chemical potentials for B and Ti. A different combination of chemical potential may result in both positive B_{Ti} and Ti_B formation energies.

Like the vacancies the antisite defects have a negligable impact on the electronic structures of the systems (see fig. 10). The electronic structure of the B_{Ti} defects resembles a lot the DOS of the Ti vacancy while the Ti_B antisite resembles the B vacancy one. This makes sense since the only difference between the vacancy and the antisite is that the atom is replaced after leaving the system.

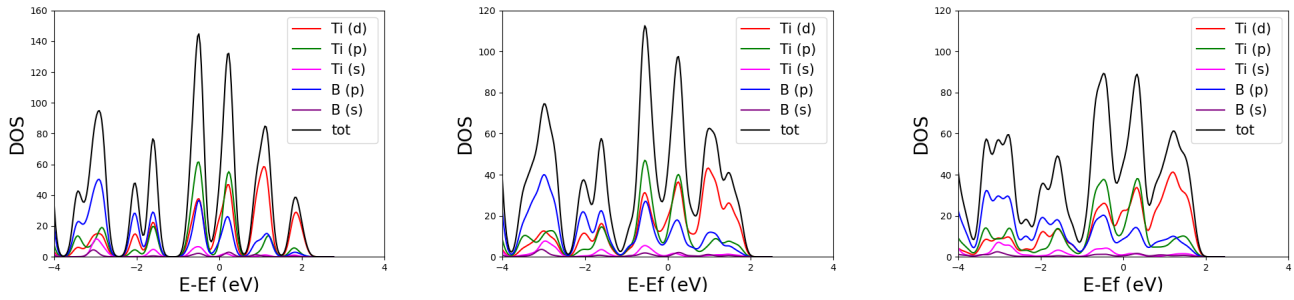

a) b) c)

Figure 10: Effects of B and Ti antisites on a 6x6x1 pristine monolayer. a) Pristine monolayer, b) B_{Ti} antisite, c) Ti_B antisite. The overall changes on the electronic structures are negligible.

4.5 Adsorption

Before calculating the adsorption energies of molecules and atoms, sites have to be chosen where the molecules are placed at the start of the simulations. Usually the sites are selected by looking at the high-symmetry points of a structure. For m-TiB_2 the chosen sites are shown in fig. 11. These sites were selected due to their high-symmetry in the m-TiB_2 structure. The tested adsorbed molecules were O_2, H_2 and H_2O since those are common in air. The molecules were placed at a distance of around 2.5Å from the adsorption sites, after which the geometry of the cell was relaxed.

a) b)

Figure 11: a) Adsorption sites on B side: bridge (between two boron atoms), top of B atom and center hexagon. b) Adsorption sites on Ti side: bridge (between two Ti atoms), top of Ti atom and center triangle. Blue dots are Ti atoms, green B atoms and orange the adsorption sites.

The adsorption energy (E_{ads}) values of a 6x6x1 cell are shown in table 6. The E_{ads} values observed for O_2 were the strongest for both the B and Ti side, where the O atoms get adsorbed at the center of the triangle for the Ti side and at the bridge site for the B side. The results also show stronger adsorption energies for the Ti side. This is probably caused by the lower electron negativity of the Ti atoms which makes them more prone to lose electrons and form bonds with oxygen. Meaning that O_2 molecules are more likely to get adsorbed if the Ti side of a monolayer faces upwards in a multilayered structure, which could lead to an increase of friction between coating and surface [18]. Having the B side facing towards air could be used as a way to reduce the adsorption of atoms and molecules since the adsorption energies are lower. Adding a layer of hexagonal boron nitride (h-BN) to the surface could further reduce the adsorption of atoms without affecting the electronic properties of the system [34]. The adsorption energies of H_2 and H_2O are lower, with center hexagon (E_{ads}= -0.08 eV) and top B atom (E_{ads} = -0.38 eV) being the most stable ones on the B side, and center triangle (E_{ads}=-2.52 eV) and Ti bridge (E_{ads}= -1.28 eV) being the most stable

ones on the Ti side for H_2 and H_2O respectively. These values come close to the values found by G. Volonakis *et al* [36] for $b\text{-}TiB_2$.

Table 6: Adsorption energies (eV) of molecules at different sites on a 6x6x1 cell.

Sides	Sites	H_2 (eV)	O_2 (eV)	O (eV)	H_2O (eV)
B side	Top B atom	-0.07	-6.16	-3.02	-0.38
	Center hexagon	-0.08	-5.57	-3.02	-0.20
	Bridge site	-0.07	—	-3.02	-0.19
Ti side	Top Ti atom	-0.18	-10.43	-5.64	-1.12
	Centre triangle	-2.52	-11.24	-5.64	-1.17
	Bridge site	-2.31	-10.15	-5.64	-1.28

While at the start the atoms are placed on high symmetry sites it does not mean they will end up getting adsorbed there. For example while the O_2 molecule starts on top of the B atom or at the center of the hexagon, when getting adsorbed, the molecule splits up into two atoms which end up at the bridge sites between B atoms (see fig. 12). The difference in adsorption energies is caused by the different distances between atoms at the end points.

The different start and end positions of the atoms are shown in table 8 in the appendix. Since the O_2 molecule splits up the adsorption energy of single O atoms were also calculated, these were around E_{ads}= -3.02 eV and E_{ads} = -5.64 eV for the B and Ti side respectively which is around half the adsorption energy of a molecule. The adsorption of H_2, O_2 or H_2O have negligible effects on the electronic structures of the systems.

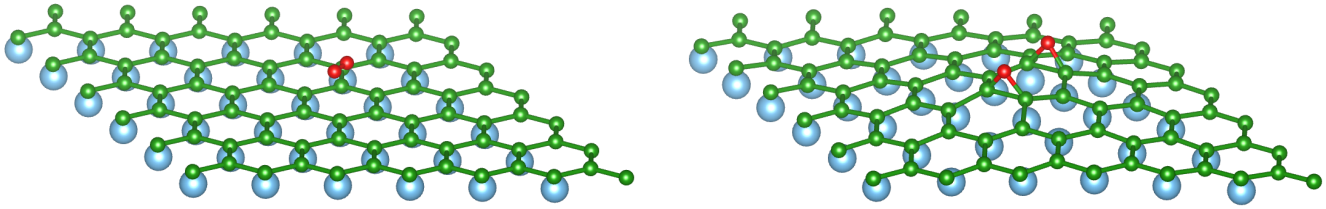

a) b)

Figure 12: Adsorption of O_2 molecule on B side. a) Start site center hexagon, b) end site bridges. Molecule splits up into two atoms when adsorbed. The two adsorbed atoms slightly bend the structure. Blue dots are Ti atoms, green B atoms and red the O atoms.

4.6 Stacking

As mentioned in section 3.6.1 the binding energies of different stacking types can hint at how a stacked TiB_2 system would shift around. The binding energies are shown in table 7

Table 7: Binding energies (eV/atom) and interlayer distances (Å) of two differently stacked monolayers and the bulk.

	Binding energy (eV/atom)	Interlayer distance (Å)
Bulk	-1.29	3.25
AA-stacked	-0.60	3.27
AB-stacked	-0.38	3.64
Bridge stacked	-0.35	3.75

The values in table 7 show that AA-stacked monolayers are the most stable systems, this indicates that the structure will probably always end up in the AA-stacked system when shifting around. The result of AA being the most stable system agrees with previously found results by Sharma *et al* [8] which showed that an AB stacked TiB_2 bilayer is dynamically and thermodynamically unstable, while an AA stacked bilayer is robust and stable.

The binding energies of 2-7 monolayers were compared and fitted in order to estimate at how many layers the structures start to become bulk-like, this was done with the AA configuration since its the most stable configuration.

$$E_{bind}(N) = \frac{a \times (2 \times E_{surface} + (N-3) \times E_{bulk})}{N} + b, \tag{15}$$

Eq. 15 is the fit used to to estimate the total number of layers required to form b-TiB_2, where $E_{surface}$, E_{bulk}, a and b are constants while N is varied. E_{bind} is the binding energy between two layers in an N layered system, $E_{surface}$ is the binding energy of one outer layer to an inner layer, E_{bulk} is the binding energy between two inner layers, N is the total number of layers in the system and a and b are initial estimated values where b is the initial estimated value for the binding energy of a single layer. For $E_{surface}$, the assumption was made that its value would be equal to the two-layered stacked structure binding energy, this because the two-layered structure consists of a single binding energy between two layers in contact with the vacuum just like the surface layer of a structure. While for E_{bulk}, the assumption was made that its value would be equal to the binding energy between two layers in b-TiB_2 which was calculated with eq. 11. Once the fit was deemed reasonable, by comparing the fitted values to the calculated ones, the data was extrapolated by letting the number of layers (N) vary between 2-100. Once the difference between the binding energy of the fit (E_{bind}) and the binding energy between two layers in a bulk (E_{bulk}) was smaller than 0.05 eV the data was considered as converged and the corresponding value N returned, which meant that the structure had become bulk-like at N layers.

Fig. 13 shows the graph of the fitted data. According to the fit the multilayered structure approaches bulk-like properties at around 29 layers (93.22 Å). The electronic structure also starts to look like the bulk as the number of layers increases (see fig.14). The results indicate that, in order to keep its weak interlayer bonds and work as a 2D layered coating, the structure needs to consist of less than 29 m-TiB_2 otherwise it will turn into the bulk material.

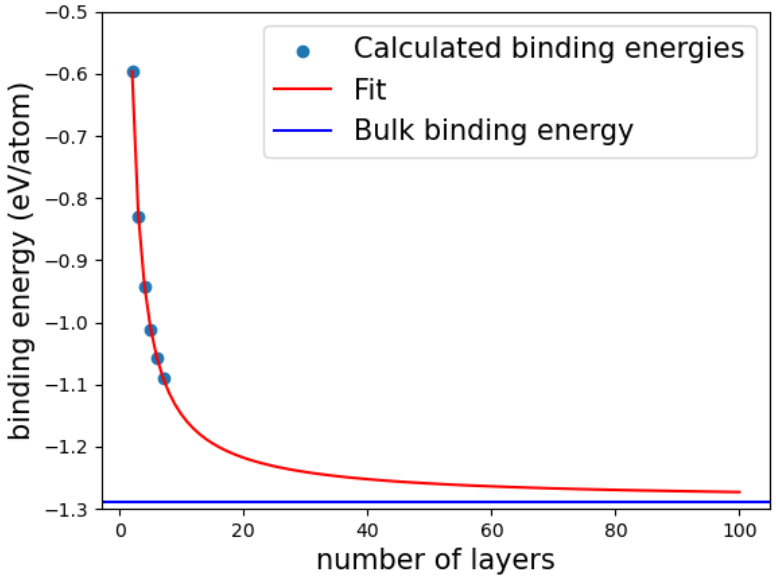

Figure 13: Fitted binding energies, x-axis number of layers, y-axis binding energy (eV/atom). Blue line represent the binding energy of the bulk while the red line is the extrapolated fit data. Once the difference between the fit data and the bulk is below 0.05 eV the layered system is considered to have become a bulk.

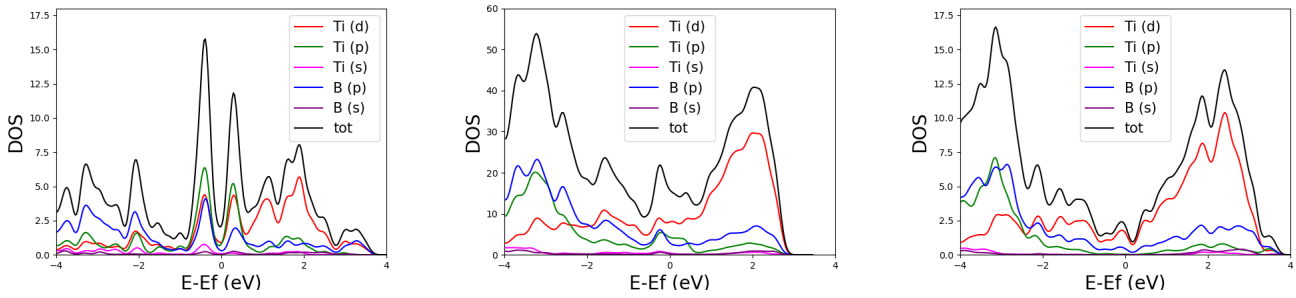

a) b) c)

Figure 14: DOS of a) monolayer, b) seven layers and c) bulk TiB_2.

5 Conclusion

In conclusion, the properties of m-TiB_2 have been looked at to determine whether stacked m-TiB_2 can be used as friction and wear resistant coating. The positive formation energy (0.23 eV/atom (PBE) and 0.26 eV/atom (optPBE-vdW)) indicates that m-TiB_2 does not form by itself and needs to be made under certain conditions with chemical or mechanical exfoliation. After formation however, m-TiB_2 is thermodinamically stable. m-TiB_2 has to be stabilized since it has a bending instability, this could be done by adding a h-BN layer on top of the monolayer. The elastic constants show an increase in strength when having more than one layer, with the AA arrangement being the strongest one. This result agrees with the calculated binding energies of the different arrangements since AA-stacking showed the strongest binding energy (E_{bind} = -0.60 eV/atom). Multiple papers report a Dirac state for m-TiB_2 this however, is not visible in our reported DOS which is probably caused by the functional used (optPBE-vdW) which underestimates band gaps. Antisite and vacancy defects both showed no significant impacts on the electronic structures of a 6x6x1 monolayer. The formation energies found for B and Ti vacancies were 0.99 eV and 1.23 eV respectively, while the formation energies for B_{Ti} and Ti_B antisites were 1.34 eV and -0.19 eV respectiveley. The negative formation energy for Ti_B antisites suggest that these would form spontaneously, this negative value is probably a result of the chosen chemical potentials for B and Ti. Subsequently the adsorption energies of H_2, O_2 and H_2O were determined. O_2 had the strongest adsorption energies -6.16 eV and -11.24 eV for the B and Ti side respectively. The adsorption of molecules and atoms has to be reduced in order for 2D TiB_2 to work as a wear and friction resistant coating. Possible ways to reduce the adsorption of molecules and atoms would be by having the B side of the monolayer facing upwards towards the air since it has the lower adsorption energy or by adding a h-BN layer on top of the structure. Finally, the total number of layers needed to go from a 2D multilayered structure to bulk-like one were calculated. This happens at around 29 layers of stacked m-TiB_2. Thus, our findings suggest that stacked m-TiB_2 could be used as a friction and wear resistant coating but with a few conditions, there has to be a protective layer (for example h-BN) which reduces the adsorption of O_2 molecules, if used as single monolayer m-TiB_2 needs to be stabilized due to its bending instability and a stacked structure needs to have less than 29 layers to keep its weak interlayer bonds and act as a 2D layered coating.

6 Future research

This study has provided insights into the properties, and potential applications of 2D TiB_2. However, several areas remain open for further investigation. Followup research could be done on, the effects a h-BN layer has on the mechanical and adsorption properties of a structure, the effects defects and adsorptions have on the mechanical properties of a structure and doping the structures to try and increase the mechanical strength.

7 Acknowledgements

I would like to thank my supervisor, Emilia Olsson and ARCNL for giving me the opportunity of doing my bachelor project with them and for all the help they provided. I would also like to thank Jon Cottom and Barsha Bhattacharjee which helped me on a daily basis and helped me stay on track when I started to lose focus of the bigger picture. I could not have had a better experience than this, I have made a lot of new friends, I have learned a lot of new things

and I can only hope to come back someday to the ARCNL family.

References

[1] K. S. Novoselov, *et al.*, Electric field effect in atomically thin carbon films, *science* **306**, 666 (2004).

[2] S. Z. Butler, *et al.*, Progress, challenges, and opportunities in two-dimensional materials beyond graphene, *ACS nano* **7**, 2898 (2013).

[3] K. S. Novoselov, A. Mishchenko, A. Carvalho, A. Castro Neto, 2d materials and van der waals heterostructures, *Science* **353**, aac9439 (2016).

[4] K. Ren, J. Yu, W. Tang, Two-dimensional zno/bse van der waals heterostructure used as a promising photocatalyst for water splitting: A dft study, *Journal of Alloys and Compounds* **812**, 152049 (2020).

[5] S. Zhang, *et al.*, Two-dimensional heterostructures and their device applications: progress, challenges and opportunities, *Journal of Physics D: Applied Physics* **54**, 433001 (2021).

[6] P. M. Das, Nanostructure engineering in two-dimensional materials beyond graphene, Ph.D. thesis, University of Pennsylvania (2020).

[7] Y. Han, *et al.*, Exploring the potential of mb 2 mbene family as promising anodes for li-ion batteries, *RSC advances* **14**, 11112 (2024).

[8] A. Sharma, A. Thakur, V. Rangra, Excitonic effects on the optical spectra of tib2 nanosheets, *Journal of Physics: Condensed Matter* **36**, 045501 (2023).

[9] R. G. Munro, Material properties of titanium diboride, *Journal of Research of the National institute of standards and Technology* **105**, 709 (2000).

[10] L. Zhang, Z. Wang, S. Du, H.-J. Gao, F. Liu, Prediction of a dirac state in monolayer tib 2, *Physical Review B* **90**, 161402 (2014).

[11] C. Sevik, J. Bekaert, M. Petrov, M. V. Milošević, High-temperature multigap superconductivity in two-dimensional metal borides, *Physical Review Materials* **6**, 024803 (2022).

[12] A. Sharma, V. Rangra, A. Thakur, Synthesis, properties, and applications of mbenes (two-dimensional metal borides) as emerging 2d materials: a review, *Journal of Materials Science* **57**, 12738 (2022).

[13] V. G. Nair, *et al.*, 2d mbenes: a novel member in the flatland, *Advanced Materials* **34**, 2108840 (2022).

[14] S. Zhang, T. Ma, A. Erdemir, Q. Li, Tribology of two-dimensional materials: From mechanisms to modulating strategies, *Materials Today* **26**, 67 (2019).

[15] K. Burke, friends, The abc of dft, *Department of Chemistry, University of California, Irvine, CA 92697* (2007).

[16] Y. Nomura, R. Akashi, Density functional theory, *arXiv preprint arXiv:2210.07647* (2022).

[17] T. Merise, On magnetic topological insulator candidate $limnsb_2te_4$, *Bachelor Thesis* (2024).

[18] J. Heimberg, K. Wahl, I. Singer, A. Erdemir, Superlow friction behavior of diamond-like carbon coatings: time and speed effects, *Applied Physics Letters* **78**, 2449 (2001).

[19] The Elastic website, `https://wolf.ifj.edu.pl/elastic/intro.html` (2018). [Online; accessed 23-May-2024].

[20] Z.-L. Liu, C. Ekuma, W.-Q. Li, J.-Q. Yang, X.-J. Li, Elastool: An automated toolkit for elastic constants calculation, *Computer Physics Communications* **270**, 108180 (2022).

[21] F. Birch, Finite elastic strain of cubic crystals, *Physical review* **71**, 809 (1947).

[22] Y. Duan, *et al.*, Elastic constants of alb2-type compounds from first-principles calculations, *Computational materials science* **51**, 112 (2012).

[23] GPAW, `https://wiki.fysik.dtu.dk/gpaw/` (2018). [Online; accessed 28-May-2024].

[24] The VASP Manual, https://www.vasp.at/wiki/index.php/The_VASP_Manual (2024). [Online; accessed 28-May-2024].

[25] M. Ernzerhof, G. E. Scuseria, Assessment of the perdew–burke–ernzerhof exchange-correlation functional, *The Journal of chemical physics* **110**, 5029 (1999).

[26] J. Klimeš, D. R. Bowler, A. Michaelides, Chemical accuracy for the van der waals density functional, *Journal of Physics: Condensed Matter* **22**, 022201 (2009).

[27] The VASP Manual, https://www.vasp.at/wiki/index.php/Nonlocal_vdW-DF_functionals (2024). [Online; accessed 8-May-2024].

[28] C. Rostgaard, The projector augmented-wave method, *arXiv preprint arXiv:0910.1921* (2009).

[29] J. Wellendorff, *et al.*, Density functionals for surface science: Exchange-correlation model development with bayesian error estimation, *Physical Review B* **85**, 235149 (2012).

[30] C. Zhang, *et al.*, Predicting novel 2d mb2 (m= ti, hf, v, nb, ta) monolayers with ultrafast dirac transport channel and electron-orbital controlled negative poisson's ratio, *The journal of physical chemistry letters* **10**, 2567 (2019).

[31] S. Grimme, Density functional theory with london dispersion corrections, *Wiley Interdisciplinary Reviews: Computational Molecular Science* **1**, 211 (2011).

[32] E. Deligoz, K. Colakoglu, Y. Ciftci, Lattice dynamical properties of scb2, tib2, and v b2 compounds, *Solid state communications* **149**, 1843 (2009).

[33] P. Spoor, *et al.*, Elastic constants and crystal anisotropy of titanium diboride, *Applied physics letters* **70**, 1959 (1997).

[34] L. Zhang, Z. Wang, S. Du, H.-J. Gao, F. Liu, Prediction of a dirac state in monolayer tib 2, *Physical Review B* **90**, 161402 (2014).

[35] J. M. Crowley, J. Tahir-Kheli, W. A. Goddard III, Resolution of the band gap prediction problem for materials design, *The journal of physical chemistry letters* **7**, 1198 (2016).

[36] G. Volonakis, L. Tsetseris, S. Logothetidis, Electronic and structural properties of tib2: Bulk, surface, and nanoscale effects, *Materials Science and Engineering: B* **176**, 484 (2011).

8 Appendix

Table 8: Table of start and end positions of H_2, O_2 and H_2O molecules. Small subscript b stands for bonded molecule while s stands for split molecule into atoms.

	Position	H_2			O_2			H_2O		
B side	Start site	top B_b	center hex_b	$bridge_b$	top B_b	center hex_b	$bridge_b$	top B_b	center hex_b	$bridge_b$
	End site	top B_b	center hex_b	$bridge_b$	$bridge_s$	$bridge_s$	—-	top B_b	center hex_b	$bridge_b$
Ti side	Start site	top Ti_b	center tri_b	$bridge_b$	top Ti_b	center tri_b	$bridge_b$	top Ti_b	center tri_b	$bridge_b$
	End site	top Ti_b	center tri_s	center tri_s	$bridge_s$	center tri_s	center tri_s	top Ti_b	top Ti_b	$bridge_b$